Review Article

Cardiovascular magnetic resonance and valvular heart diseases: a suggested protocol for congenital lesions

Francesca Baessato[1,2], Alessandro Ruzzarin[2], Christian Meierhofer[1]

[1]Congenital Heart Disease and Pediatric Cardiology, German Heart Center Munich, TUM University Hospital, Technical University of Munich, School of Medicine and Health, Munich, Germany; [2]Department of Cardiology, Regional Hospital S. Maurizio, Bolzano, Italy

Contributions: (I) Conception and design: F Baessato, C Meierhofer; (II) Administrative support: C Meierhofer; (III) Provision of study materials or patients: F Baessato, C Meierhofer; (IV) Collection and assembly of data: All authors; (V) Data analysis and interpretation: All authors; (VI) Manuscript writing: All authors; (VII) Final approval of manuscript: All authors.

Correspondence to: Dr. Francesca Baessato, MD. Department of Cardiology, Regional Hospital S. Maurizio, Via Lorenz Böhler 5, 39100 Bolzano, Italy; Congenital Heart Disease and Pediatric Cardiology, German Heart Center Munich, TUM University Hospital, Technical University of Munich, School of Medicine and Health, Munich, Germany. Email: francesca.baessato89@gmail.com.

Abstract: Valvular heart diseases (VHDs) require definition of anatomy, severity, and risk stratification to best define procedural need, type of intervention and seriate follow-up. Congenital lesions are much rarer and often associated with more complex lesions. Among noninvasive imaging modalities, cardiovascular magnetic resonance (CMR) represents a fundamental tool for complete assessment and quantification of VHDs. CMR can provide wide anatomical views on cardiac and extra-cardiac structures in any plane orientation, flow and volume quantification, as well as information on ventricular remodeling and viability. In the context of valve stenosis, quantification by CMR is based primarily on direct measurement of valve orifice at maximal valve opening, although CMR data remain less reliable than standard echocardiography due to reduced temporal resolution. Definition of great vessels anatomy by CMR can allow differentiation of valvular, subvalvular or supravalvular lesions. For valve regurgitation, CMR is the gold standard for quantification of ventricular volumes and function and for direct calculation of regurgitation of the semilunar valves with through-plane phase-contrast images. Additional flow measurements can be integrated to cross-check quantitative data on great vessels flow and stroke volumes. A standardized approach is recommended in CMR studies. A minimum CMR dataset should include two-dimensional cine and phase-contrast sequences, and three-dimensional whole heart imaging. This should be applied in the clinical practice to assess VHDs, including most complex congenital lesions.

Keywords: Cardiovascular magnetic resonance (CMR); valvular heart diseases (VHDs); congenital lesions

Submitted Sep 18, 2024. Accepted for publication Mar 24, 2025. Published online Apr 23, 2025.
doi: 10.21037/cdt-24-470
View this article at: https://dx.doi.org/10.21037/cdt-24-470

Introduction

Valvular heart diseases (VHDs) are common in the general population (1). Besides bicuspid aortic valves, congenital causes for VHDs are rare, but progression of surgical and interventional procedures have led to significant improvement of survival and long-term outcomes as well as need for follow-up in the last decades (2). Noninvasive imaging modalities are essential for diagnosis and follow-up of VHDs and are routinely performed to quantify the severity of valve lesions and define patients' management. Echocardiography is traditionally considered the standard tool to evaluate VHDs, thanks to its wide availability, low cost, safety and easy performance. This imaging modality can provide very good visualization of the anatomy of the valvular and subvalvular apparatus and excellent functional analysis. Moreover, echocardiography complements anatomical and functional data with

assessment of hemodynamic features such as estimation of pulmonary pressures and effects during exercise. Recently developed strain analysis and three-dimensional (3D) echocardiography have been added to improve its diagnostic and prognostic abilities (3,4). However, principal concerns of echocardiography in the assessment of VHDs are its dependence on acoustic windows, interobserver variability, lack of myocardial tissue characterization, need for geometric and hemodynamic assumptions and for a multiparametric approach to provide quantification of disease severity (5). This often makes definition of disease severity qualitative, especially for valve regurgitation, which limits a standardized reporting and valuable follow-up (6). In the last few years, cardiac computed tomography (CCT) has also emerged as a valid tool to evaluate VHDs, especially in the presence of extensive valve calcifications and in the procedural planning phase (7). However, its role in children is mainly limited by radiation exposure as well as potential lack of flow data in standard CCT protocols and quantitative data on volume quantification provided by last generation CCT scanners are not routinely applied in the clinical practice yet (8).

Among noninvasive imaging modalities, cardiovascular magnetic resonance (CMR) can significantly complement echocardiography in the diagnosis and prognosis of VHDs, thanks to its excellent ability to provide quantitative data, especially for valve regurgitation (9). Main advantages of CMR are its lack of ionizing radiation, low operator dependency and high reproducibility, possibility to provide wide anatomical planes and 3D views of valves and their surrounding cardiac structures, including anatomy of the great vessels (10). Moreover, CMR can identify focal or diffuse pathological myocardial alterations due to replacement fibrosis or inflammation in chronic VHDs, which may be evident already at young age (11). Specific CMR features of primary cardiomyopathies, myocardial overload and ischemic heart diseases may be evident in both parametric mapping and late gadolinium enhancement sequences and should be considered to help differential diagnosis with myocardial alterations secondary to pure VHDs.

CMR is considered the gold standard for quantification of ventricular volumes and function and is more accurate than echocardiography in the presence of multiple valve lesions (1,11-13). Overall, CMR has been recommended as a class I imaging modality for long-term follow-up in various adult congenital heart diseases (14). Major limitations of CMR are its longer acquisition times and costs. In the context of VHDs, CMR is generally recommended when echocardiographic data are doubtful or insufficient, and when calculation of aortic and pulmonary regurgitation is needed along with the diameters of aorta and pulmonary trunk (7). Current guidelines for VHDs are mainly based on echocardiographic studies (1), while specific CMR data for severity and indications for intervention are still lacking; but, hopefully, ongoing CMR studies will close this gap in a near future. Aim of this review is to highlight the role of CMR in the field of VHDs targeted to define presence and entity of lesions and to provide a standardized approach for CMR studies even for complex congenital lesions.

Recommended CMR protocol for VHDs

Evaluation of VHDs is based on standard CMR sequences, that we recommend in every CMR protocol for assessment of valve lesions, as shown in *Table 1*.

2D steady-state free-precession (SSFP) cine imaging can provide both anatomical and functional data and is fundamental to accurately visualize the valvular and subvalvular apparatus, as well as the outflow/inflow tracts of both ventricles with no restriction of imaging planes, independently from cardiac and thoracic anatomy. 2D-SSFP cine imaging allows good visualization of both stenotic and regurgitant jets. High-velocity jets, due to either stenotic or regurgitant valve lesions, typically present a central, bright, signal surrounded by dark signal voids, that relate to laminar and turbulent blood flow, respectively. Spoiled gradient echo sequences can be used as an alternative to 2D SSFP, as they are less susceptible to flow turbulence and metal artefacts. An example is shown in *Figure 1*. For calculation of ventricular volumes, mass and function, multiphase 2D SSFP cine with breath hold and retrospective electrocardiogram (ECG)-gating are acquired in a stack of multiple, contiguous slices in the short-axis or axial planes (15). We recommend a slice thickness of 6 mm (children) or 8 mm (adults) and zero gap. As valvular and subvalvular structures are thin, a reduced slice thickness to 4 or 5 mm can be set for better assessment of valve anatomy, although CMR remains limited compared to echocardiography in visualization of very small and mobile structures such as valvular vegetations due to insufficient temporal resolution or out-of-plane movement (16,17).

We recommend performance of 3D whole heart sequences to provide anatomical data on cardiac and thoracic anatomy to detect any concomitant congenital lesion. These sequences are frequently applied in children as they do not require breath-holding or contrast medium

Table 1 Suggested standard and additional cardiovascular magnetic resonance sequences for assessment of congenital valvular heart diseases

CMR sequences	Focus on
Standard	
2D SSFP	- Anatomical and functional data with visualization of valve opening, structural changes of the valvular and subvalvular apparatus, and presence of stenotic or regurgitant jets
	- Quantification of ventricular volumes, mass and function
	- Indirect calculation of mitral and tricuspid valve regurgitation (from ventricular stroke volumes)
	- Direct planimetry of valve orifice at maximal opening for quantification of valve stenosis
3D whole heart	- Wide anatomical data on cardiac and extra-cardiac anatomy
2D PC	- Direct quantification of regurgitant volume and regurgitant fraction (through-plane imaging)
	- Measurement and visualization of peak flow velocity (through-plane imaging: maximal velocity at imaging level; in-plane imaging: maximal velocity along the stenotic jet)
Additional	
4D flow	- Assessment of flow volume and velocity in 3 dimensions
	- Direct visualization of flow pattern and vortices
Parametric mapping	- Normal or diffuse increase of native T1 and ECV values
Late gadolinium enhancement	- Identification of presence, pattern and extension of myocardial fibrosis

CMR, cardiovascular magnetic resonance; ECV, extracellular volume; PC, phase-contrast; SSFP, steady-state free precession.

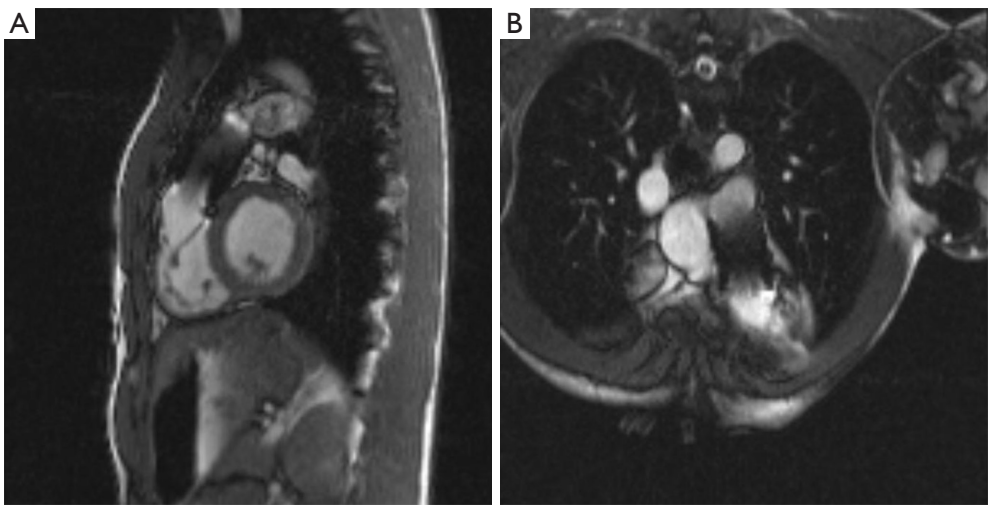

Figure 1 A Sapien valve implanted in the right ventricular outflow tract. Metal artifacts are evident in both (A) longitudinal and (B) en face views on 2D balanced steady-state-free-precession cine. For such patients, imaging at 1.5 T is preferable rather than 3 T and spoiled gradient echo sequences can be performed as are less affected by susceptibility artifacts.

(18,19). A breathing navigator prospectively acquires images at a defined phase of the respiratory cycle, thus reducing breathing artefacts. A retrospective ECG trigger is set to acquire images at a specific phase of the cardiac cycle, thus reducing blurring artefacts due to cardiac structures and vessel motion. These sequences are limited by metallic artefacts in the presence of stents or prothesis, and relatively long acquisition times (15). As an alternative, gadolinium-enhanced 3D magnetic resonance angiography can be performed for vessel assessment with acquisition of

images in a single breath-hold. However, usually no ECG-triggering is applied with resulting blurring artefacts and contrast medium is needed (gadolinium) (20).

2D phase-contrast (PC) sequences have shown good accuracy and reproducibility for flow quantification (21,22). Temporal resolution of CMR is typically 25 to 45 ms, which is significantly lower than that of doppler echocardiography. This may significantly limit assessment of high velocity jets and consequently direct measurement of peak flow velocity in stenotic lesions (23). Most reliable quantitative data for assessment of valve stenosis by CMR are based on direct planimetry of the valve orifice measured in an anatomical plane acquired through the valve tips at maximal valve opening, rather than on measurement of peak velocity and valve gradient (24,25). Standard acquisition planes are set on the ascending aorta, main pulmonary trunk and right and left pulmonary arteries, although any additional plane can be derived from dedicated 2D cine or 3D whole heart images (26). Setting of a proper velocity encoding rate (VENC) is needed to avoid aliasing artefacts due to high velocity regurgitation jets or concomitant valve stenoses. Baseline phase offset errors due to inhomogeneities in the magnetic field can be limited by applying phantom correction and automated baseline correction tools with current commercial analysis software (27). For regurgitant VHDs, through-plane 2D PC sequences are planned perpendicular to flow direction and allow direct measurement of regurgitant volume and regurgitant fraction. For stenotic VHDs, in-plane 2D PC sequences planned along flow direction allow direct measurement of peak flow velocity and can demonstrate the site of stenosis very well. However, CMR peak velocities remain underestimated due to limited temporal and spatial resolution, which depends on voxel size.

4D flow sequences have been introduced in the last decade as an alternative to standard 2D PC sequences. Main advantages are that 4D flow can allow measurements of blood flow (volume, velocity) in 3 dimensions simultaneously, with wide visualization of complex flow patterns in the great vessels, it does not rely on accurate planification of acquisition planes and is not affected by tortuous jets or valve motion throughout the cardiac cycle (28). Measurements of wall shear stress and wall pressures can also be given (29). However, main limitations are represented by relatively long acquisition and post-processing times. Recently published consensus papers have encouraged and facilitated widespread adoption of 4D flow, beyond a pure role confined to the research area, although it is currently not routinely performed in all CMR centers (30,31).

Additionally, tissue characterization with myocardial mapping and late gadolinium enhancement can be performed to detect any myocardial alteration due to chronic overload of VHDs.

Semilunar valves

Aortic and pulmonary stenosis

Assessment of aortic and pulmonary stenosis with CMR is based on anatomical and functional imaging of the ventricular outflow tracts and of the ascending aorta or pulmonary arteries, respectively. This is fundamental to correctly identify the site of stenosis (subvalvular, valvular, supravalvular). In case of stenosis at valve level, a good visualization of the semilunar valves "en face" is recommended to assess its morphology (unicuspid, bicuspid, tricuspid, quadricuspid), structural changes and opening (32). Diameters of the aortic root and pulmonary arteries should be routinely reported (33). Concerning quantitative data, direct planimetry of the valve orifice, measured on cine imaging at end-systole at valve tips, is considered the most reliable method to quantify the severity of stenosis. Of note, CMR planimetry has shown high sensitivity and specificity among other non-invasive imaging modalities when compared to cardiac catheterization and is very reliable and reproducible (34). There are no specific cut-off values for CMR, and generally the same thresholds for echocardiography are applied. A valve area <1.0 cm^2 is indicative of severe aortic or pulmonary stenosis. Due to low accuracy, measurement of transvalvular peak velocity with 2D PC imaging may be added (35), although we do not recommend reporting it as a standard. Presence and pattern of ventricular hypertrophy should also be reported. Diffuse elevation of native T1 and extracellular volume values may be detected, as well as diffuse, intramyocardial fibrosis. These are present especially in the most hypertrophied myocardial segments and correlate with patients' prognosis (36-38).

Bicuspid aortic valve is the most frequent congenital VHD. It may remain silent for years or evolve into valve degeneration with cusps calcification and thickening, leading to valve incompetence, stenosis or both (39). Discerning pure stenosis at valvular level from supra- or subvalvular aortic stenosis is crucial for definition of type and timing of intervention. The Ross operation has been increasingly adopted in the last years in the pediatric population as an alternative to prosthetic valves. CMR covers a central role

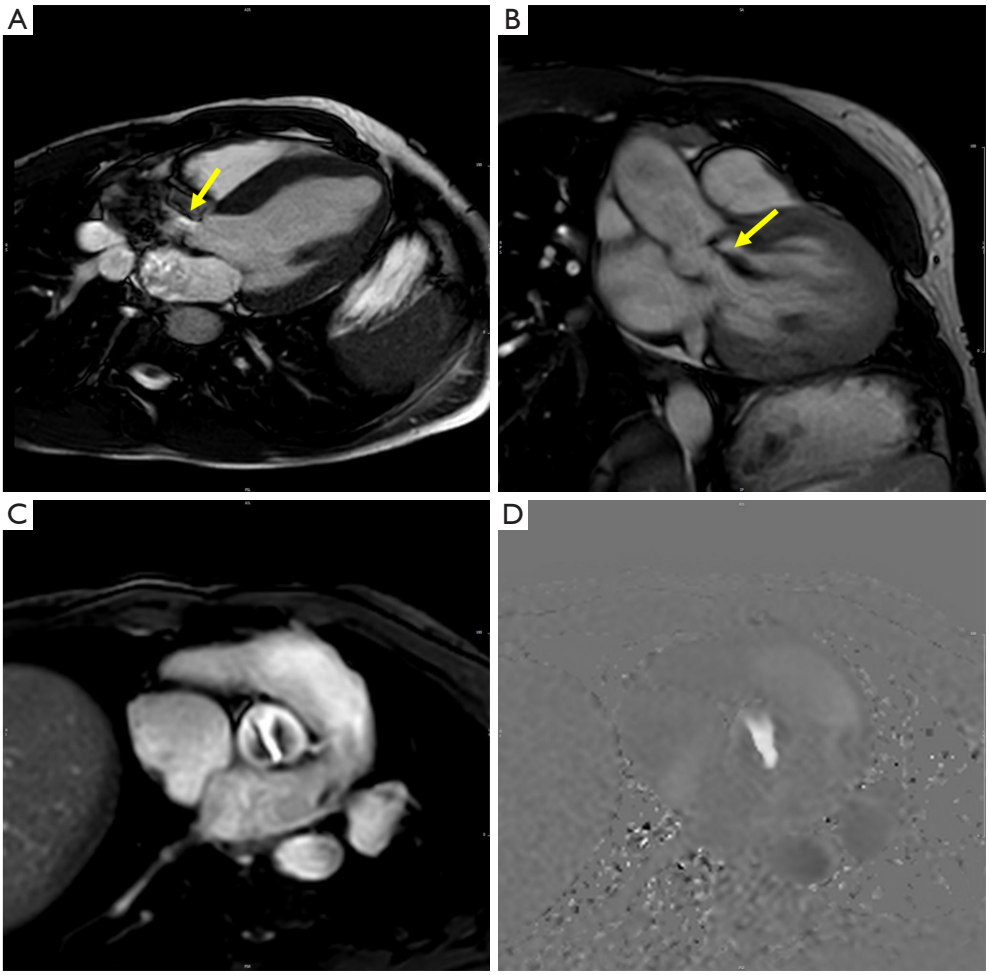

Figure 2 A 25-year-old patient, male. A high acceleration jet (yellow arrows) due to combined aortic stenosis and regurgitation is demonstrated in two-dimensional steady-state-free-precession images (A,B). En face view at valve level in both cine and phase-contrast sequences reveals a bicuspid morphology of the aortic valve (C,D).

in the planning procedural phase and in the assessment of long-term complications, such as pulmonary autograft dilatation and subsequent aortic regurgitation (40). *Figure 2* shows an example of a mixed lesion at aortic valve level due to bicuspid morphology.

An example of supravalvular pulmonary stenosis is given in *Figure 3*. Surgical repair of transposition of the great arteries is based on arterial switch and includes the LeCompte maneuver. Here the pulmonary trunk is translocated anterior to the ascending aorta and supravalvular pulmonary stenosis may occur as postoperative complication (41) (*Figure 3*).

Aortic and pulmonary regurgitation

CMR represents a cornerstone in the quantification of aortic (AR) and pulmonary (PR) regurgitation, given its high accuracy (42) and reproducibility (43) when compared to standard tools such as echocardiography. This is particularly valuable for PR, due to the more complex geometry of the right ventricle compared to the left ventricle and the more anterior position of the pulmonary valve, which is often difficult to assess with echocardiography (1).

Flow data are assessed with 2D PC sequences, ideally planned with through-plane imaging just above the aortic

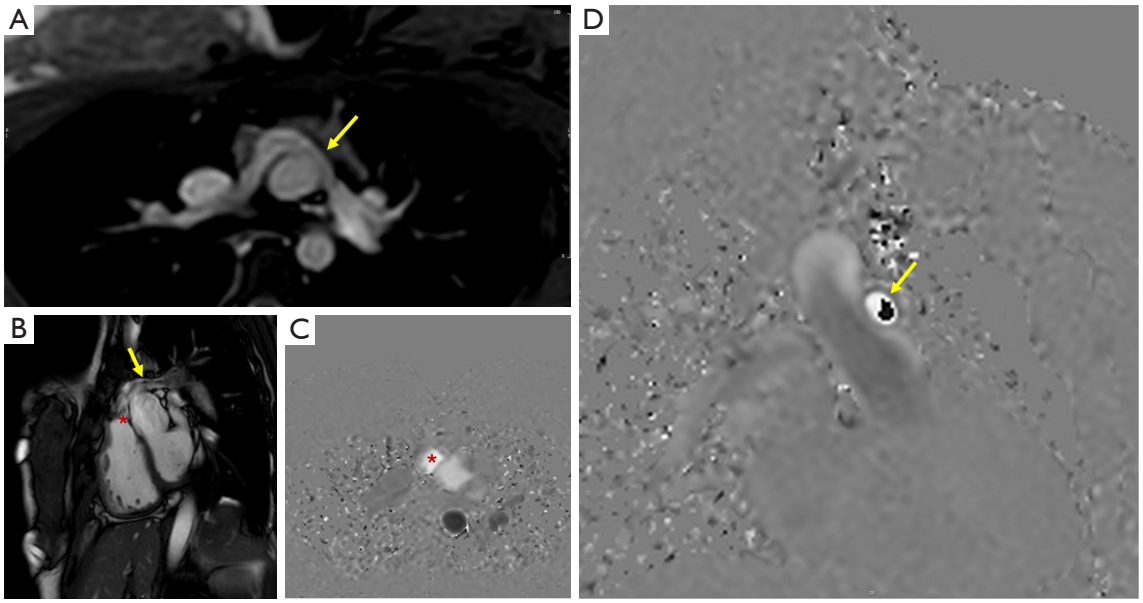

Figure 3 A 19-year-old patient, female with transposition of the great arteries with intact interventricular septum after arterial switch. In the localizer sequences (A) the pulmonary trunk appears anterior to the ascending aorta after LeCompte maneuver, and suspect arises for stenosis at the proximal left pulmonary artery (yellow arrow). Cine imaging demonstrates acceleration across the vessel (B, yellow arrow). In two-dimensional phase contrast sequences, no aliasing occurs using a standard VENC of 200 at pulmonary valve level (C, red star), while a significant aliasing occurs using the same VENC at the origin of the left pulmonary artery (D, yellow arrow), confirming the presence of stenosis at supravalvular level. VENC, velocity encoding rate.

and pulmonary valve. Various studies demonstrated high heterogeneity in AR quantification when performed at valve level or above at the ascending aorta (44). In the presence of relevant AR, measurement in the ascending aorta with 2D flow may significantly overestimate AR severity, due to multiple vortexes that develop in the aortic root, which is often dilated (45). In these cases, acquisition of 2D PC in multiple imaging planes including the aortic annulus, the sino-tubular junction and the proximal ascending aorta can be addressed to provide and compare more quantitative data. Preferably, measurements in proximity to valve level should be adopted as have shown greater reproducibility and lower heterogeneity (38). Additionally, 2D PC flow measurement in the descending aorta or at diaphragmatic level can reveal holodiastolic flow reversal as a suggestive sign for severe AR. In the presence of metal objects such as stents or conduits, flow imaging should be planned just above or below them to avoid wrong measurements due to dephasing.

Direct quantitative data measured in the ascending aorta and pulmonary artery can be compared to the left and right ventricular stroke volume, respectively, when no shunt or valve insufficiency is present. Flow calculation in the pulmonary veins, caval veins, descending aorta and pulmonary arteries may also be used for a double check. Presence of concomitant ventricular dilatation and eccentric hypertrophy should also be reported, as well as accurate measures of the ascending aorta and pulmonary trunk. Presence, extension and type of aortic aneurysms should also be assessed and described in clinical reports for serial follow-up. Tissue characterization sequences may reveal subtle myocardial scarring and add prognostic data in patients with chronic aortic regurgitation (46).

Cut-off values for VHDs severity by CMR have been reported, but heterogeneity remains, among consensus papers, to define quantitative ranges for mild, moderate and severe lesions (1,39). Currently, CMR cut-off data are validated only for PR, where a regurgitation fraction of ≥40% is considered severe (47,48). For AR, a threshold of >35–40% has been proposed for severe regurgitation, but is based mainly on echocardiographic data and on adverse outcomes assessed in observational studies (1). Eventually, AR regurgitant fraction may be strongly influenced by

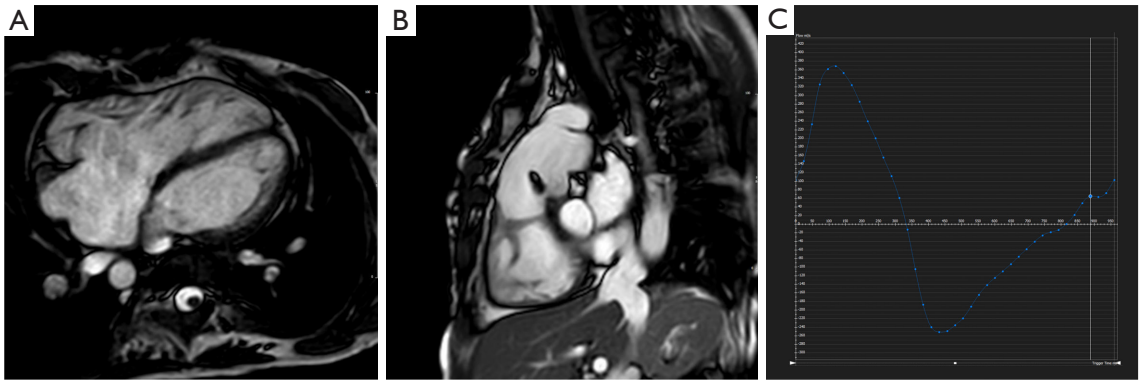

Figure 4 A 50-year-old patient, female, with diagnosis of repaired tetralogy of Fallot. (A,B) Relevant dilatation of the right cardiac chambers in long-axis and short-axis planes, respectively. Free pulmonary regurgitation results secondary to reconstruction of the right ventricular outflow tract with a Goretex patch. A regurgitant volume of 52 mL with a regurgitant fraction of 59% are calculated in the post-processing phase from two-dimensional phase contrast images acquired at pulmonary trunk level (C).

hemodynamic and patient's parameters such as heart rate, concomitant use of vasodepressors, blood pressure and physical activity (49). In the context of congenital cardiac lesions, one of the most common findings in repaired tetralogy of Fallot is severe PR. This occurs secondary to surgery where the right ventricular outflow tract is enlarged, eventually with a transanular patch and monocuspid valve (50). Pulmonary valve replacement can be performed in selected cases and CMR covers a central role for the identification of valuable candidates for interventional valve repair (15) (*Figure 4*).

Atrio-ventricular valves

Mitral and tricuspid stenosis

Similarly to the semilunar valves, quantitative assessment of mitral and tricuspid stenosis is based on direct planimetry of valve orifice at maximal valve opening (end-diastole) and a valve orifice <1.0 cm^2 is considered indicative of severe mitral stenosis (51). Again, accurate positioning of the image plane perpendicular to the valve tips is essential to not over- or underestimate data. Qualitative assessment relies on 2D cine imaging to assess restricted movement of valve leaflets and their morphological characteristics, with a dedicated stack of parallel slices or long-axis views through the valves. In such cases, presence of thickened, calcified valve leaflets may even help valve tracking.

Mitral regurgitation (MR) and tricuspid regurgitation (TR)

Quantification of MR and TR with CMR is based on both 2D PC and 2D SSFP cine imaging. The most applied method is based on calculation of the regurgitant volume as the difference of the left or right ventricular stroke volume (derived from volume quantification in cine imaging) and the aortic or pulmonary flow (directly measured with through-plane 2D PC sequences) (indirect method). In the presence of any AR or PR, the regurgitant volume of the semilunar valve should be counted and calculated out of the stroke volume to not underestimate TR or MR. This method has demonstrated very high reproducibility and accuracy when compared to echocardiography (52). Alternatively, the regurgitant volume can be derived from the difference of the stroke volumes of the right and left ventricle using cine imaging. However, in the presence of multiple valve lesions or intracardiac shunts, this method could not be applied (53). Significant advantages of both approaches are that they are independent from regurgitant jet number or direction and do not rely on geometric assumptions or need for contrast agents (54). Imprecise measurement of ventricular stroke volumes due to arrhythmias, breathing artifacts or incorrect post-processing analysis may significantly affect data reliability.

Direct through-plane 2D PC images on the mitral and tricuspid valve can provide direct measurement of the

regurgitant volume, although this method may be affected by the continuous motion of the valve annulus plane during systole. Additionally, high velocities regurgitant jets may result in aliasing or lead to underestimation of diastolic flow and overestimation of the regurgitant fraction (55). Accurate valve tracking is performed in the post-processing phase first on a single image and then automatically propagated through all images in the cardiac cycle to allow manual correction and software analysis. In the presence of very eccentric or multiple jets, direct quantification of valve regurgitation by 2D PC imaging may be challenging, as a single image plane should be planned just perpendicular to the regurgitant jet to not underestimate data (56). Qualitative assessment of MR and TR can be achieved with a stack of multiple, thin, contiguous slices planned perpendicular to valve commissures to identify coaptation points and structural changes with cine imaging. An axial stack is ideal to entirely assess the anatomy of the tricuspid valve. Long-axis planes through valve leaflets are helpful to confirm presence of valve prolapse. Although transesophageal echocardiography is considered the gold standard for definition of mitral valve anatomy and leaflet alterations, CMR is useful when echo windows are insufficient, and quantification of disease severity remains uncertain (15,57). Moreover, a prognostic impact of entity of MR as quantified by CMR has been demonstrated in various studies, which is helpful to give indication for early surgery even in asymptomatic patients (58,59). In addition, CMR studies can reveal presence and entity of mitral valve annulardisjunction (MAD), which is suggestive for higher arrhythmic risk and prognosis. Further prospective studies are needed to define the role of MAD for patients' management (60).

Among congenital causes for TR, Ebstein's anomaly is rare and results from apical displacement of the functional annulus of the tricuspid valve. The septal and posterior leaflets of the tricuspid valve fail to delaminate from the native myocardium during the embryologic evolution, leading to atrialization of a part of the right ventricle. Consequently, TR occurs and results in volume overload and dilatation of the functional right ventricle. This chronic overload may lead to global myocardial alterations and systolic dysfunction (2,61). The CMR study is targeted to quantify the volume and function of the functional right ventricle, the dimensions (volume, area) of the right atrium and the severity of TR as regurgitant volume and regurgitant fraction in native Ebstein's anomaly patients (*Figure 5*). Displacement of valve leaflets should also be reported. Any associated congenital heart defect (atrial and ventricular septal defects) should be additionally assessed (62). CMR is also fundamental to assess the impact of cone procedure in operated Ebstein's anomaly patients in terms of reduction of tricuspid regurgitation and right cardiac chambers volume overload (*Figure 6*).

A frequent cause for MR is mitral valve prolapse. CMR plays a central role in stratifying patients' risk by definition of MR severity, entity of ventricular dilatation and dysfunction, presence of ventricular fibrosis and mitral annular disjunction (63,64) (*Figure 7*).

Conclusions

CMR is a fundamental tool for diagnosis, interventional planning and serial follow-up of many VHDs, including most congenital lesions. A standardized approach is needed in the acquisition, post-processing and reporting of any CMR study, especially when complex lesions are documented. Due to high heterogeneity in grading of VHDs, we recommend to always specify real quantitative data (e.g., percentage of regurgitation fraction) in the CMR clinical report.

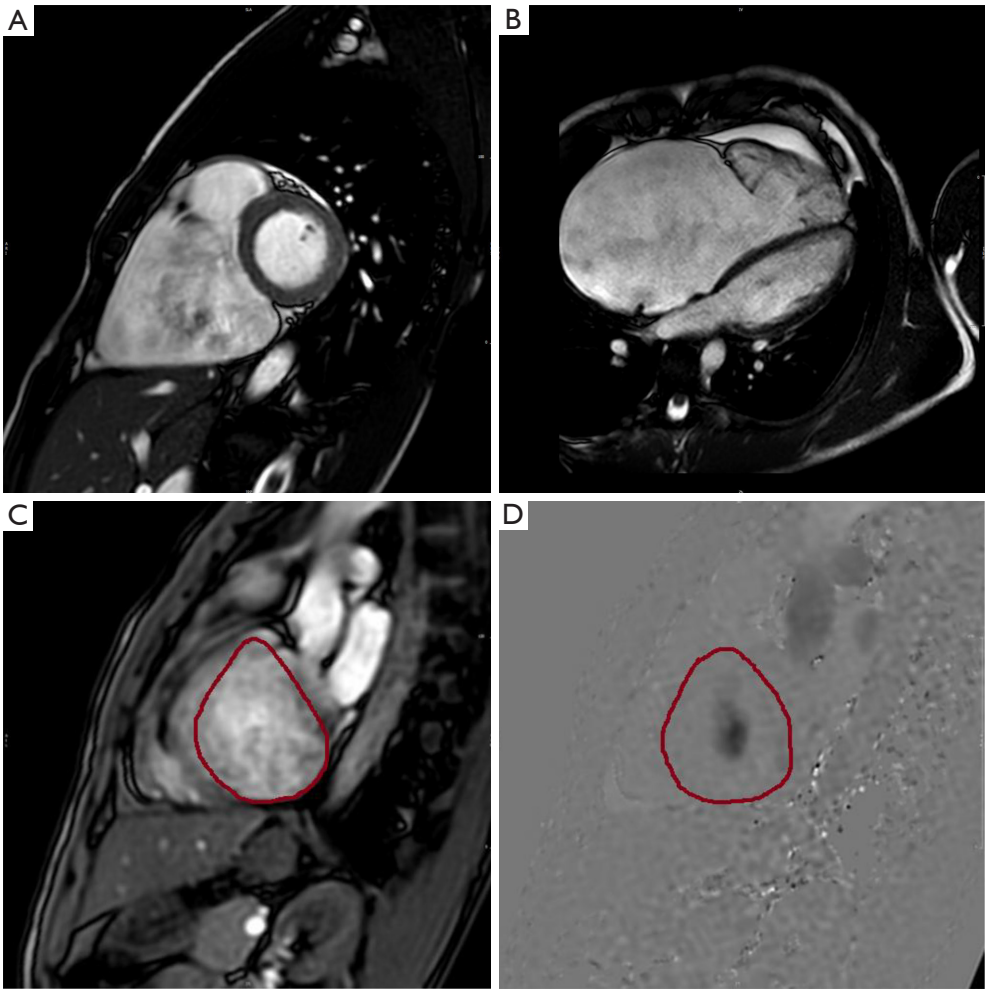

Figure 5 A 19-year-old patient, male. Significant right ventricular atrialization as a consequence of apical displacement of the tricuspid valve in Ebstein's anomaly (A,B). En face view of the tricuspid valve in both cine and phase contrast images (C,D) allows direct quantification of tricuspid regurgitation.

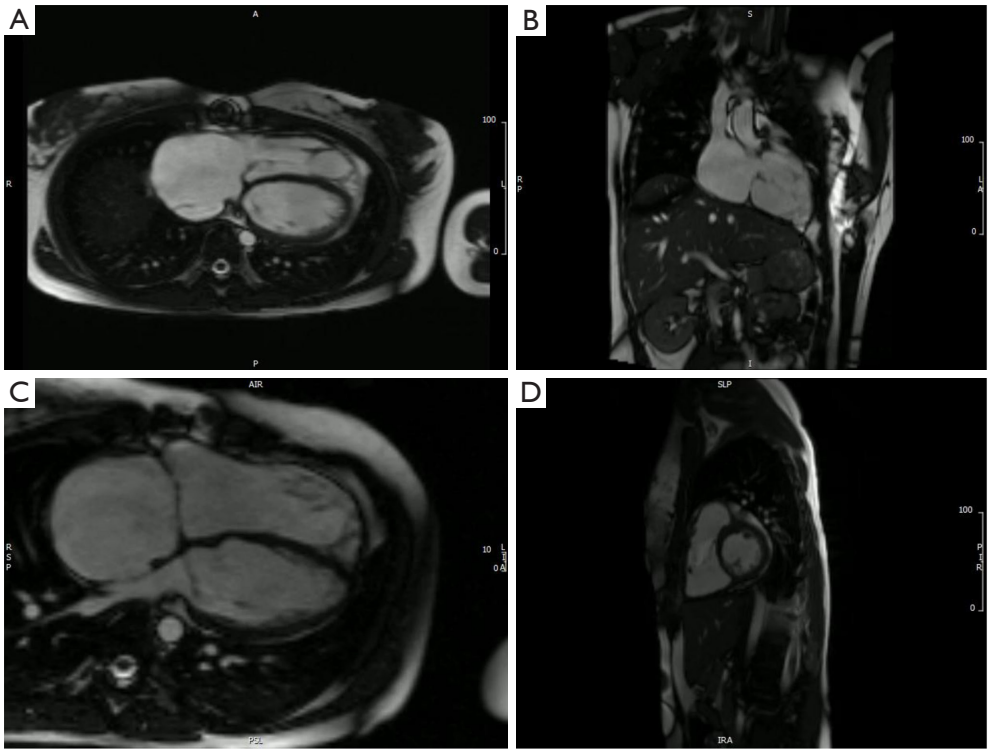

Figure 6 A 22-year-old patient, female, with Ebstein's anomaly and cone repair of the tricuspid valve. Surgical reconstruction of the tricuspid valve at the anatomical annulus resembles a cone-shape in cine imaging. A significant reduction of tricuspid regurgitation is intuitive in both long-axis (A-C) and short-axis (D) cine planes.

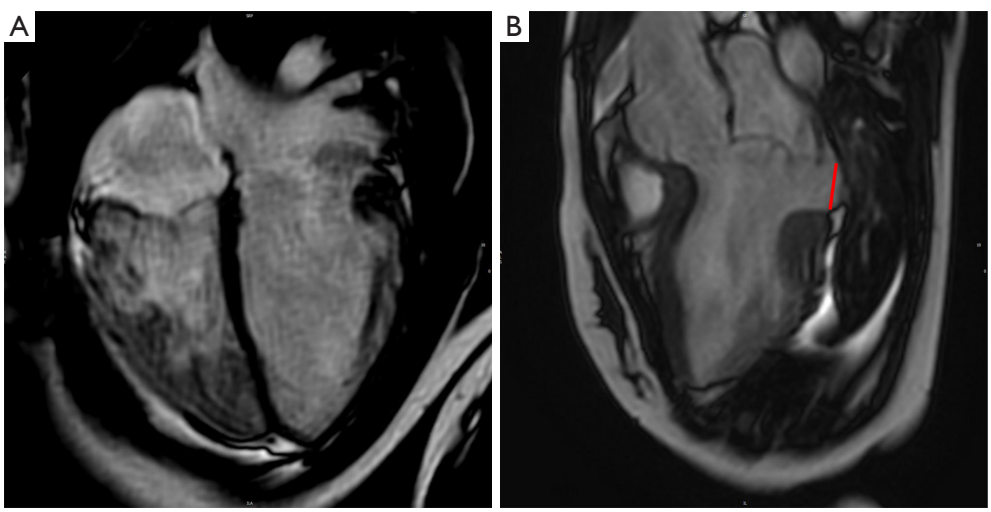

Figure 7 A 15-year-old patient, female, affected by Marfan syndrome. Mitral valve prolapse with severe mitral regurgitation is evident in (A) four-chamber and (B) three-chamber views. Mitral annular disjunction can be measured as the distance between the posterior mitral valve leaflet and the left atrial wall at end-systole (B, red line).

Acknowledgments

None.

Footnote

Provenance and Peer Review: This article was commissioned by the Guest Editor (Harald Kaemmermer) for the series "Current Management Aspects in Adult Congenital Heart Disease (ACHD): Part VI" published in *Cardiovascular Diagnosis and Therapy*. The article has undergone external peer review.

Peer Review File: Available at https://cdt.amegroups.com/article/view/10.21037/cdt-24-470/prf

Funding: None.

Conflicts of Interest: All authors have completed the ICMJE uniform disclosure form (available at https://cdt.amegroups.com/article/view/10.21037/cdt-24-470/coif). The series "Current Management Aspects in Adult Congenital Heart Disease (ACHD): Part VI" was commissioned by the editorial office without any funding or sponsorship. The authors have no other conflicts of interest to declare.

Ethical Statement: The authors are accountable for all aspects of the work in ensuring that questions related to the accuracy or integrity of any part of the work are appropriately investigated and resolved.

References

1. Myerson SG. CMR in Evaluating Valvular Heart Disease: Diagnosis, Severity, and Outcomes. JACC Cardiovasc Imaging 2021;14:2020-32.
2. Edwards JE. Pathologic features of ebstein's malformation of the tricuspid valve. Proc Staff Meet Mayo Clin 1952;28:89-94.
3. Radmilovic J, D'Andrea A, D'Amato A, et al. Echocardiography in Athletes in Primary Prevention of Sudden Death. J Cardiovasc Echogr 2019;29:139-48.
4. Springhetti P, Tomaselli M, Benfari G, et al. Peak atrial longitudinal strain and risk stratification in moderate and severe aortic stenosis. Eur Heart J Cardiovasc Imaging 2024;25:947-57.
5. Zoghbi WA, Adams D, Bonow RO, et al. Recommendations for Noninvasive Evaluation of Native Valvular Regurgitation: A Report from the American Society of Echocardiography Developed in Collaboration with the Society for Cardiovascular Magnetic Resonance. J Am Soc Echocardiogr 2017;30:303-71.
6. Bartko PE, Arfsten H, Heitzinger G, et al. A Unifying Concept for the Quantitative Assessment of Secondary Mitral Regurgitation. J Am Coll Cardiol 2019;73:2506-17.
7. Doherty JU, Kort S, Mehran R, et al. ACC/AATS/AHA/ASE/ASNC/HRS/SCAI/SCCT/SCMR/STS 2017 Appropriate Use Criteria for Multimodality Imaging in Valvular Heart Disease: A Report of the American College of Cardiology Appropriate Use Criteria Task Force, American Association for Thoracic Surgery, American Heart Association, American Society of Echocardiography, American Society of Nuclear Cardiology, Heart Rhythm Society, Society for Cardiovascular Angiography and Interventions, Society of Cardiovascular Computed Tomography, Society for Cardiovascular Magnetic Resonance, and Society of Thoracic Surgeons. J Am Coll Cardiol 2017;70:1647-72.
8. Conte E, Mushtaq S, Muscogiuri G, et al. The Potential Role of Cardiac CT in the Evaluation of Patients With Known or Suspected Cardiomyopathy: From Traditional Indications to Novel Clinical Applications. Front Cardiovasc Med 2021;8:709124.
9. Baessato F, Fusini L, Muratori M, et al. Echocardiography vs. CMR in the Quantification of Chronic Mitral Regurgitation: A Happy Marriage or Stormy Divorce? J Cardiovasc Dev Dis 2023;10:150.
10. Fratz S, Chung T, Greil GF, et al. Guidelines and protocols for cardiovascular magnetic resonance in children and adults with congenital heart disease: SCMR expert consensus group on congenital heart disease. J Cardiovasc Magn Reson 2013;15:51.
11. Baggiano A, Del Torto A, Guglielmo M, et al. Role of CMR Mapping Techniques in Cardiac Hypertrophic Phenotype. Diagnostics (Basel) 2020;10:770.
12. Pontone G, Guaricci AI, Andreini D, et al. Prognostic

Benefit of Cardiac Magnetic Resonance Over Transthoracic Echocardiography for the Assessment of Ischemic and Nonischemic Dilated Cardiomyopathy Patients Referred for the Evaluation of Primary Prevention Implantable Cardioverter-Defibrillator Therapy. Circ Cardiovasc Imaging 2016;9:e004956.
13. Burchfield JS, Xie M, Hill JA. Pathological ventricular remodeling: mechanisms: part 1 of 2. Circulation 2013;128:388-400.
14. Baumgartner H, De Backer J, Babu-Narayan SV, et al. 2020 ESC Guidelines for the management of adult congenital heart disease. Eur Heart J 2021;42:563-645.
15. Baessato F, Ewert P, Meierhofer C. CMR and Percutaneous Treatment of Pulmonary Regurgitation: Outreach the Search for the Best Candidate. Life (Basel) 2023;13:1127.
16. Bellenger NG, Burgess MI, Ray SG, et al. Comparison of left ventricular ejection fraction and volumes in heart failure by echocardiography, radionuclide ventriculography and cardiovascular magnetic resonance; are they interchangeable? Eur Heart J 2000;21:1387-96.
17. Thiele H, Paetsch I, Schnackenburg B, et al. Improved accuracy of quantitative assessment of left ventricular volume and ejection fraction by geometric models with steady-state free precession. J Cardiovasc Magn Reson 2002;4:327-39.
18. François CJ, Tuite D, Deshpande V, et al. Unenhanced MR angiography of the thoracic aorta: initial clinical evaluation. AJR Am J Roentgenol 2008;190:902-6.
19. Hussain T, Lossnitzer D, Bellsham-Revell H, et al. Three-dimensional dual-phase whole-heart MR imaging: clinical implications for congenital heart disease. Radiology 2012;263:547-54.
20. Geva T, Greil GF, Marshall AC, et al. Gadolinium-enhanced 3-dimensional magnetic resonance angiography of pulmonary blood supply in patients with complex pulmonary stenosis or atresia: comparison with x-ray angiography. Circulation 2002;106:473-8.
21. Hundley WG, Li HF, Hillis LD, et al. Quantitation of cardiac output with velocity-encoded, phase-difference magnetic resonance imaging. Am J Cardiol 1995;75:1250-5.
22. Chatzimavroudis GP, Oshinski JN, Franch RH, et al. Evaluation of the precision of magnetic resonance phase velocity mapping for blood flow measurements. J Cardiovasc Magn Reson 2001;3:11-9.
23. Woldendorp K, Bannon PG, Grieve SM. Evaluation of aortic stenosis using cardiovascular magnetic resonance: a systematic review & meta-analysis. J Cardiovasc Magn Reson 2020;22:45.
24. John AS, Dill T, Brandt RR, et al. Magnetic resonance to assess the aortic valve area in aortic stenosis: how does it compare to current diagnostic standards? J Am Coll Cardiol 2003;42:519-26.
25. Tanaka K, Makaryus AN, Wolff SD. Correlation of aortic valve area obtained by the velocity-encoded phase contrast continuity method to direct planimetry using cardiovascular magnetic resonance. J Cardiovasc Magn Reson 2007;9:799-805.
26. Varaprasathan GA, Araoz PA, Higgins CB, et al. Quantification of flow dynamics in congenital heart disease: applications of velocity-encoded cine MR imaging. Radiographics 2002;22:895-905; discussion 905-6.
27. Chernobelsky A, Shubayev O, Comeau CR, et al. Baseline correction of phase contrast images improves quantification of blood flow in the great vessels. J Cardiovasc Magn Reson 2007;9:681-5.
28. Hope TA, Markl M, Wigström L, et al. Comparison of flow patterns in ascending aortic aneurysms and volunteers using four-dimensional magnetic resonance velocity mapping. J Magn Reson Imaging 2007;26:1471-9.
29. Minderhoud SCS, Arrouby A, van den Hoven AT, et al. Regional aortic wall shear stress increases over time in patients with a bicuspid aortic valve. J Cardiovasc Magn Reson 2024;26:101070.
30. Westenberg JJ, Roes SD, Ajmone Marsan N, et al. Mitral valve and tricuspid valve blood flow: accurate quantification with 3D velocity-encoded MR imaging with retrospective valve tracking. Radiology 2008;249:792-800.
31. Bissell MM, Raimondi F, Ait Ali L, et al. 4D Flow cardiovascular magnetic resonance consensus statement: 2023 update. J Cardiovasc Magn Reson 2023;25:40.
32. Saef JM, Ghobrial J. Valvular heart disease in congenital heart disease: a narrative review. Cardiovasc Diagn Ther 2021;11:818-39.
33. Kramer CM, Barkhausen J, Flamm SD, et al. Standardized cardiovascular magnetic resonance (CMR) protocols 2013 update. J Cardiovasc Magn Reson 2013;15:91.
34. Kupfahl C, Honold M, Meinhardt G, et al. Evaluation of aortic stenosis by cardiovascular magnetic resonance imaging: comparison with established routine clinical techniques. Heart 2004;90:893-901.
35. Kilner PJ, Manzara CC, Mohiaddin RH, et al. Magnetic resonance jet velocity mapping in mitral and aortic valve stenosis. Circulation 1993;87:1239-48.
36. Everett RJ, Treibel TA, Fukui M, et al. Extracellular Myocardial Volume in Patients With Aortic Stenosis. J Am

Coll Cardiol 2020;75:304-16.
37. Musa TA, Treibel TA, Vassiliou VS, et al. Myocardial Scar and Mortality in Severe Aortic Stenosis. Circulation 2018;138:1935-47.
38. Debl K, Djavidani B, Buchner S, et al. Delayed hyperenhancement in magnetic resonance imaging of left ventricular hypertrophy caused by aortic stenosis and hypertrophic cardiomyopathy: visualisation of focal fibrosis. Heart 2006;92:1447-51.
39. Thiene G, Rizzo S, Basso C. Bicuspid aortic valve: The most frequent and not so benign congenital heart disease. Cardiovasc Pathol 2024;70:107604.
40. Cattapan C, Della Barbera M, Dedja A, et al. Mechanical and Structural Adaptation of the Pulmonary Root after Ross Operation in a Murine Model. J Clin Med 2022;11:3742.
41. Moscatelli S, Avesani M, Borrelli N, et al. Complete Transposition of the Great Arteries in the Pediatric Field: A Multimodality Imaging Approach. Children (Basel) 2024;11:626.
42. Søndergaard L, Lindvig K, Hildebrandt P, et al. Quantification of aortic regurgitation by magnetic resonance velocity mapping. Am Heart J 1993;125:1081-90.
43. Dulce MC, Mostbeck GH, O'Sullivan M, et al. Severity of aortic regurgitation: interstudy reproducibility of measurements with velocity-encoded cine MR imaging. Radiology 1992;185:235-40.
44. Chatzimavroudis GP, Oshinski JN, Pettigrew RI, et al. Quantification of mitral regurgitation with MR phase-velocity mapping using a control volume method. J Magn Reson Imaging 1998;8:577-82.
45. Gerhardt P, Shehu N, Ferrari I, et al. Quantifying aortic valve regurgitation in patients with congenital aortic valve disease by 2D and 4D flow magnetic resonance analysis. Int J Cardiol 2024;408:132084.
46. Malahfji M, Senapati A, Tayal B, et al. Myocardial Scar and Mortality in Chronic Aortic Regurgitation. J Am Heart Assoc 2020;9:e018731.
47. Kawel-Boehm N, Hetzel SJ, Ambale-Venkatesh B, et al. Reference ranges ("normal values") for cardiovascular magnetic resonance (CMR) in adults and children: 2020 update. J Cardiovasc Magn Reson 2020;22:87. Erratum in: J Cardiovasc Magn Reson 2021;23:114.
48. Rebergen SA, Chin JG, Ottenkamp J, et al. Pulmonary regurgitation in the late postoperative follow-up of tetralogy of Fallot. Volumetric quantitation by nuclear magnetic resonance velocity mapping. Circulation 1993;88:2257-66.
49. Stern H, Calavrezos L, Meierhofer C, et al. Physical exercise reduces aortic regurgitation: exercise magnetic resonance imaging. JACC Cardiovasc Imaging 2014;7:314-5.
50. Stellin G, Guariento A, Vida VL. Evolving Techniques for the Achievement of Optimal Long-Term Results After Tetralogy of Fallot Repair. World J Pediatr Congenit Heart Surg 2021;12:116-23.
51. Djavidani B, Debl K, Lenhart M, et al. Planimetry of mitral valve stenosis by magnetic resonance imaging. J Am Coll Cardiol 2005;45:2048-53.
52. Le Goffic C, Toledano M, Ennezat PV, et al. Quantitative Evaluation of Mitral Regurgitation Secondary to Mitral Valve Prolapse by Magnetic Resonance Imaging and Echocardiography. Am J Cardiol 2015;116:1405-10.
53. Underwood SR, Klipstein RH, Firmin DN, et al. Magnetic resonance assessment of aortic and mitral regurgitation. Br Heart J 1986;56:455-62.
54. Fujita N, Chazouilleres AF, Hartiala JJ, et al. Quantification of mitral regurgitation by velocity-encoded cine nuclear magnetic resonance imaging. J Am Coll Cardiol 1994;23:951-8.
55. Lopez-Mattei JC, Shah DJ. The role of cardiac magnetic resonance in valvular heart disease. Methodist Debakey Cardiovasc J 2013;9:142-8.
56. Krieger EV, Lee J, Branch KR, et al. Quantitation of mitral regurgitation with cardiac magnetic resonance imaging: a systematic review. Heart 2016;102:1864-70.
57. Stork A, Franzen O, Ruschewski H, et al. Assessment of functional anatomy of the mitral valve in patients with mitral regurgitation with cine magnetic resonance imaging: comparison with transesophageal echocardiography and surgical results. Eur Radiol 2007;17:3189-98.
58. Penicka M, Vecera J, Mirica DC, et al. Prognostic Implications of Magnetic Resonance-Derived Quantification in Asymptomatic Patients With Organic Mitral Regurgitation: Comparison With Doppler Echocardiography-Derived Integrative Approach. Circulation 2018;137:1349-60.
59. Uretsky S, Gillam L, Lang R, et al. Discordance between echocardiography and MRI in the assessment of mitral regurgitation severity: a prospective multicenter trial. J Am Coll Cardiol 2015;65:1078-88.
60. Van der Bijl P, Stassen J, Haugaa KH, et al. Mitral Annular Disjunction in the Context of Mitral Valve Prolapse: Identifying the At-Risk Patient. JACC Cardiovasc Imaging 2024;17:1229-45.
61. Müller J, Kühn A, Tropschuh A, et al. Exercise

performance in Ebstein's anomaly in the course of time - Deterioration in native patients and preserved function after tricuspid valve surgery. Int J Cardiol 2016;218:79-82.
62. Fratz S, Janello C, Müller D, et al. The functional right ventricle and tricuspid regurgitation in Ebstein's anomaly. Int J Cardiol 2013;167:258-61.
63. Garg P, Swift AJ, Zhong L, et al. Assessment of mitral valve regurgitation by cardiovascular magnetic resonance imaging. Nat Rev Cardiol 2020;17:298-312.
64. Basso C, Iliceto S, Thiene G, et al. Mitral Valve Prolapse, Ventricular Arrhythmias, and Sudden Death. Circulation 2019;140:952-64.

Cite this article as: Baessato F, Ruzzarin A, Meierhofer C. Cardiovascular magnetic resonance and valvular heart diseases: a suggested protocol for congenital lesions. Cardiovasc Diagn Ther 2025;15(2):441-454. doi: 10.21037/cdt-24-470